BRIEF COMMUNICATION

Behaviour of carbon and boron impurities in the Madison Symmetric Torus

S T A Kumar[1]**, D J Den Hartog**[1]**, R M Magee**[1]**, G Fiksel**[1,3] **and D Craig**[2]

[1] Department of Physics, University of Wisconsin-Madison, Madison, WI, USA
[2] Wheaton College, Wheaton, IL, USA

E-mail: stkumar@wisc.edu

Abstract
Temporally and spatially resolved measurements of carbon and boron impurity density are obtained in the reversed field pinch (RFP) for the first time. It is observed that, unlike in tokamaks and stellarators, the RFP does not exhibit a centrally peaked impurity profile in either standard plasmas where field lines have some degree of stochasticity, or improved confinement discharges where there exist well-nested flux surfaces for a substantial fraction of the plasma volume. Results from improved confinement discharges also indicate an outward convection of impurities from the core of the plasma.

It is well known that plasma–wall interaction in fusion devices liberates impurities [1]. Deliberate injection of impurities at the edge of the plasma has also been applied in many fusion devices as a method to reduce heat load to the wall by forming a radiative edge [2]. Transport of these edge impurities in the plasma is governed by the electric field and thermal forces. Collisional (neoclassical) theory predicts that these edge impurities have a natural tendency to accumulate in the core of the plasma [3]. This has been experimentally observed in many experiments in high confinement regimes [4–7]. This poses a serious concern as these impurities can have deleterious effects on the performance of a fusion device such as fuel dilution and increased radiative loss. In the reversed field pinch (RFP), the global magnetic reconnection activities enhance plasma–wall interactions and liberate impurities into the plasma [8]. A good understanding of impurity generation and transport is crucial for RFP operation. Even though there exists a large number of theoretical and experimental studies on tokamaks and stellarators, there is a paucity of time-resolved and spatially localized information about impurities in RFP plasmas. Impurity studies in RFPs have been supported by line integrated emission measurements [9–12]. A large range in the transport parameters in different machines is found in these works.

[3] Currently at the Laboratory for Laser Energetics, University of Rochester, NY, USA.

In this paper, we present the first temporally and spatially resolved impurity density measurements in the Madison Symmetric Torus (MST) RFP (major radius $R = 1.5$ m, minor radius $a = 0.52$ m) [13]. Measurements of fully stripped boron and carbon impurities are obtained using charge-exchange recombination spectroscopy (CHERS). Experimental observations indicate a flat/weakly hollow impurity density profile for standard plasma discharges. Sawtooth (global magnetic reconnection) events in standard discharges result in a significant increase and the radial redistribution of impurities. (A description of sawtooth events in MST and their impact on main plasma parameters is available in previous publications. For example, see [14].) In improved confinement discharges, the hollowness of the radial profile increases, and the core impurity density slowly decays in time concurrent with an increase in impurity density in the outer regions of the plasma, indicating an outward impurity convection. The reason for this outward convection is not clear.

Experiments are conducted in deuterium plasmas of toroidal plasma current ∼400 kA, line averaged central electron density $n_e \sim (0.8–1) \times 10^{19}$ m^{-3} and central electron temperature ranging from 400 eV (in standard discharges) to above 1 keV (in improved confinement discharges). Improved confinement discharges are achieved by the 'pulsed poloidal current drive' (PPCD) scheme [15]. The main characteristics of PPCD discharges are low levels of magnetic fluctuations, higher core electron temperature and improved energy confinement [16–18]. Major sources of carbon impurity in MST are toroidal and poloidal graphite limiters. Recent boronization efforts in MST resulted in increased boron levels in the plasma.

Measurements of carbon and boron impurities are done by collecting C VI emission at $\lambda = 343.4$ nm ($n = 7$ to $n = 6$ transition) and B V emission at $\lambda = 298.1$ nm ($n = 6$ to $n = 5$ transition), respectively. These emissions are stimulated by charge exchange between fully stripped ions and 50 keV hydrogen atoms injected radially using neutral beam injector. Distinct features of CHERS on MST are good spatial (∼2 cm) resolution and a dynamic background subtraction for good temporal resolution (up to 100 kHz) [19–21]. The spectrometer has recently been calibrated for radiant sensitivity using a tungsten–halogen lamp for absolute impurity density calculations from charge-exchange emission brightness. (A 10% uncertainty is estimated in the impurity density, mainly due to uncertainties in the beam attenuation calculations and transmission efficiencies of the viewing lenses.)

Radial and temporal profiles of C^{6+} density are shown in figures 1(a) and (b), respectively. Data are averaged over a large number of sawtooth events. Profiles away (∼1.5 ms before) from the sawtooth event represent equilibrium profiles. The C^{6+} density has a flat/weakly hollow profile both at and away from the event. There is a global increase in the C^{6+} density at sawtooth events. The 'burst' of impurity density at a sawtooth event is more apparent from the sawtooth averaged temporal evolution shown in figure 1(b). The chord at $\rho \sim 0.75$, where ρ is the radial distance from the magnetic axis normalized to the plasma minor radius, shows the maximum increase, which is consistent with the fact that sawtooth activity leads to the liberation of impurities from the wall. Impurities injected at a sawtooth event are expelled before the subsequent event.

The radial profile of C^{6+} density for PPCD discharges shown in figure 2(a) indicates a clearly hollow profile and a steep gradient at $\rho \sim 0.6$. Temporal behaviour of the C^{6+} density at three radial locations ($\rho \sim 0.02$, 0.55 and 0.76) is plotted in figure 2(b). A slow decay of the core impurity density in time after the transition to improved confinement is apparent. The impurity density at the outer regions of the plasma, on the other hand, is slowly increasing. Measurements of B^{5+} density also show similar behaviour for both standard and PPCD discharges, as shown in figure 3.

Standard discharges in MST have multiple, coupled tearing modes and the magnetic field lines have some degree of stochasticity for most of the plasma volume. Therefore, the flat
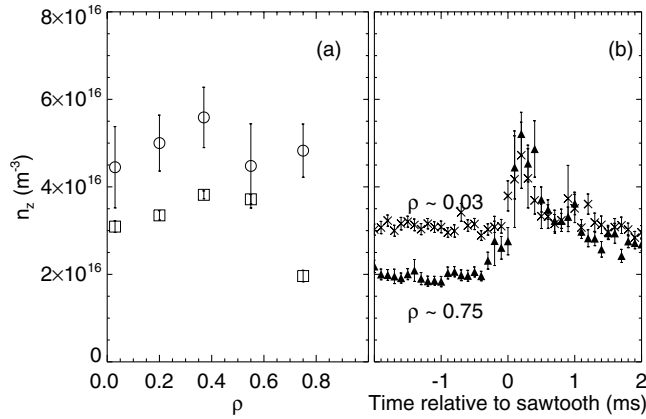
Figure 1. C^{6+} density for standard discharges: (*a*) radial profiles away from ($\square$) and at ($\bigcirc$) sawtooth events. (*b*) Sawtooth averaged temporal evolution at $\rho \sim 0.03$ and $\rho \sim 0.75$. Error-bars show standard deviation of the mean from ensembles.
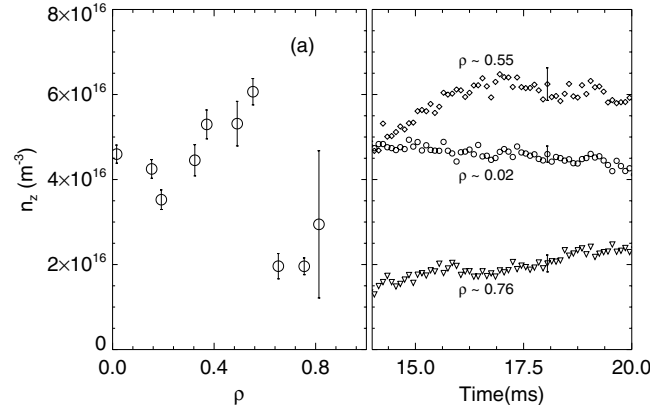
Figure 2. C^{6+} density for PPCD discharges: (*a*) radial profile and (*b*) temporal evolution after transition to improved confinement at three radial locations: core($\rho \sim 0.02$), mid-radius($\rho \sim 0.55$) and outer regions ($\rho \sim 0.76$) of the plasma. Data are averaged over similar discharges. Error-bars represent standard deviation of the mean from samples.

impurity density profile in standard discharges is not a surprising result, as stochasticity leads to mixing of different plasma regions. However, the impurity 'burst' observed at a sawtooth event is somewhat surprising. At a sawtooth event, the electron temperature decreases by ~ 50–100 eV, and the neutral hydrogen density increases by almost an order of magnitude. The decrease in electron temperature leads to a reduced ionization rate, and the increase in neutral density to an increased level of charge-exchange loss of fully stripped impurities. This should result in a drop in the density of fully stripped impurities in the plasma. In contrast, we observe a burst in the impurity density at a sawtooth event. It is likely that there is a huge influx of impurities from the wall and an increase in the inward stochastic transport during a sawtooth event, which overcomes the low ionization rate and increased charge-exchange loss. The observation of an increase in the C III emission during sawteeth in MST [14] reinforces

3
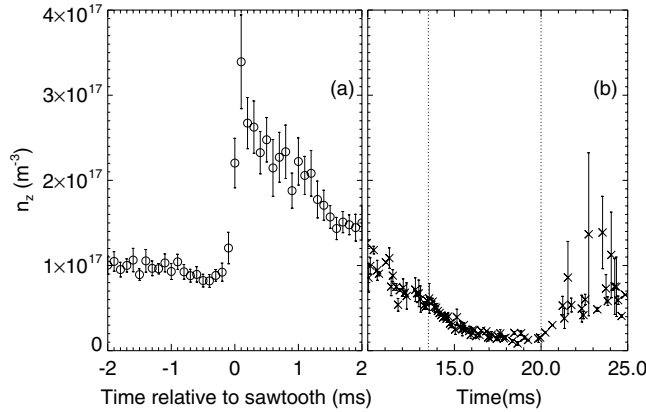
Figure 3. Temporal evolution of B^{5+} density at core for standard (*a*) and improved confinement (*b*) discharges. Region between dotted lines represents duration of good confinement regime for figure (*b*).

the supposition that increased plasma–wall interactions at sawtooth events inject impurities into the plasma. This is consistent with other observations in the RFP, of enhanced impurity influx during dynamo activity due to increased plasma–wall interactions [8, 22]. This was attributed to sputtering due to high energy ions and charge-exchange neutrals generated at sawtooth activity, at the wall.

Our calculations on ionization balance of carbon and boron impurities using the Atomic Data Analysis Structure (ADAS) [23] show that, for standard discharges, lower ionization states of carbon and boron are available throughout the plasma, whereas in PPCD discharges, these light impurities are fully stripped in the core region ($0 < \rho \leqslant 0.6$). Therefore, unlike standard discharges, for the PPCD regime, the measured impurity density is the total content of that impurity in the plasma for the core region. This is supported by the experimental observation of a slow decay in the core impurity density during PPCD, even though the core electron temperature is increasing. The decrease in core impurity density, concurrent with a slow increase in impurity density in the outer regions of the plasma, indicates the presence of an impurity expulsion mechanism. The impurity decay time, calculated from the exponential fit to the core impurity decay, averaged over many similar discharges, is $\sim 31.5 \pm 1.5$ ms, which is much larger than the energy confinement time of ~ 10 ms in PPCD discharges [16]. Following Rowan *et al* [24], the spatial scale length of the impurity density profile can be taken as a good measure of the 'impurity peaking factor' ($\frac{v_r}{D}$, where D is the diffusion coefficient and v_r is the convection velocity), which is naturally positive for our hollow profile (~ 1.5 m^{-1} at $\rho \sim 0.5$). A positive peaking factor indicates positive v_r, i.e. an outward convection. The observed large gradient in the impurity density at $\rho \sim 0.6$ of the PPCD plasma is consistent with the previous observation of steep gradients in ion and electron temperatures in PPCD plasmas near $\rho \sim 0.6$ [16, 25]. This may be an indication of barrier formation, but more work is necessary to draw any conclusion.

The mechanism of outward convection of impurities and possible barrier formation in PPCD plasmas is not clear at present. As the magnetic fluctuations are reduced in this regime, electrostatic fluctuations could be a likely candidate for transport. The possibility of temperature screening of impurities [3] cannot be ruled out as we have a strong ion temperature gradient and a nearly flat ion density profile (inferred from electron density profile). A detailed investigation of possible mechanisms is not in the scope of this paper.

In conclusion, this paper presents experimental studies of light impurities in the Madison Symmetric Torus reversed field pinch. High resolution localized impurity density measurements on MST indicate a flat/weakly hollow radial profile in standard discharges with a strong impurity burst at sawtooth events. Improved confinement discharges exhibit increased hollowness and outward impurity convection.

Acknowledgments

References

[1] McCracken G M, Fielding S J, Matthews G F and Pitcher C S 1989 Impurity production due to wall interactions in tokamaks *J. Nucl. Mater.* **162–164** 392–7

[2] Ongena J *et al* and Zastrow K-D EFDA-JET workprogramme contributors 2001 Recent progress toward high performance above the greenwald density limit in impurity seeded discharges in limiter and divertor tokamaks *Phys. Plasmas* **8** 2188–98

[3] Hirshman S P and Sigmar D J 1981 Neoclassical transport of impurities in tokamak plasmas *Nucl. Fusion* **21** 1079

[4] Dux R, Giroud C, Neu R, Peeters A G, Stober J and Zastrow K-D and Contributors to the EFDA-JET Workprogramme 2003 Accumulation of impurities in advanced scenarios *J. Nucl. Mater.* **313–316** 1150–5 (Plasma-Surface Interactions in Controlled Fusion Devices 15)

[5] Petrasso R D, Sigmar D J, Wenzel K W, Hopf J E, Greenwald M, Terry J L and Parker J 1986 Observations of centrally peaked impurity profiles following pellet injection in the Alcator-*C* tokamak *Phys. Rev. Lett.* **57** 707–10

[6] Smeulders P *et al* 1995 Survey of pellet enhanced performance in JET discharges *Nucl. Fusion* **35** 225

[7] Ida K, Fonck R J, Sesnic S, Hulse R A, Leblanc B and Paul S F 1989 Impurity behavior in PBX L- and H-mode plasmas *Nucl. Fusion* **29** 231–50

[8] Matsuoka A, Masamune S, Nagata A, Arimoto H, Yamada S, Murata H, Oshiyama H and Sato K I 1989 Plasma–wall interactions in a reversed-field pinch *J. Nucl. Mater.* **162** 804–11

[9] Carolan P G, Patel A, Sexton M C and Walsh M J 1990 First measurements of the particle confinement in a reversed field pinch by the laser ablation method *Nucl. Fusion* **30** 2616–21

[10] Menmuir S, Carraro L, Alfier A, Bonomo F, Fassina A, Spizzo G and Vianello N 2010 Impurity transport studies in RFX-mod multiple helicity and enhanced confinement QSH regimes *Plasma Phys. Control. Fusion* **52** 095001

[11] Carraro L, Puiatti M E, Sattin F, Scarin P, Valisa M and Mattioli M 1996 Carbon and oxygen behaviour in the reversed field pinch RFX *Nucl. Fusion* **36** 1623

[12] Kuldkepp M, Brunsell P R, Cecconello M, Dux R, Menmuir S and Rachlew E 2006 Measurements and modeling of transport and impurity radial profiles in the EXTRAP T2R reversed field pinch *Phys. Plasmas* **13** 092506

[13] Dexter R N, Kerst D W, Lovell T W, Prager S C and Sprott J C 1991 The Madison Symmetric Torus *Fusion Technol.* **19** 131–9

[14] Chapman B E, Almagri A F, Cekic M, Den Hartog D J, Prager S C and Sarff J S 1996 Sawteeth and energy confinement in the Madison Symmetric Torus reversed-field pinch *Phys. Plasmas* **3** 709–11

[15] Sarff J S, Hokin S A, Ji H, Prager S C and Sovinec C R 1994 Fluctuation and transport reduction in a reversed field pinch by inductive poloidal current drive *Phys. Rev. Lett.* **72** 3670–3

[16] Chapman B E and *et al* 2002 High confinement plasmas in the Madison Symmetric Torus reversed-field pinch *Phys. Plasmas* **9** 2061–8

[17] Franz P, Marrelli L, Piovesan P, Chapman B E, Martin P, Predebon I, Spizzo G, White R B and Xiao C 2004 Observations of multiple magnetic islands in the core of a reversed field pinch *Phys. Rev. Lett.* **92** 125001

[18] O'Connell R *et al* 2003 Observation of velocity-independent electron transport in the reversed field pinch *Phys. Rev. Lett.* **91** 045002

[19] Den Hartog D J and *et al* 2006 Advances in neutral-beam-based diagnostics on the Madison Symmetric Torus reversed-field pinch (invited) *Rev. Sci. Instrum.* **77** 10F122

[20] Craig D, Den Hartog D J, Ennis D A, Gangadhara S and Holly D 2007 High throughput spectrometer for fast localized doppler measurements *Rev. Sci. Instrum.* **78** 013103

[21] Gangadhara S, Craig D, Ennis D A and Den Hartog D J 2006 Modeling fast charge exchange recombination spectroscopy measurements from the Madison Symmetric Torus *Rev. Sci. Instrum.* **77** 10F109

[22] Kamada Y, Arimoto H, Yamada S, Nagashima K, Matsuoka A, Sato K and Inoue N 1987 Enhancement of impurity influx due to the dynamo action in RFP plasma *J. Phys. Soc. Japan* **56** 859–62

[23] Summers H P 2004 *The Adas User Manual, version 2.6* www.adas.ac.uk

[24] Rowan W L, Bespamyatnov I O and Fiore C L 2008 Light impurity transport at an internal transport barrier in alcator c-mod *Nucl. Fusion* **48** 105005

[25] Chapman B E *et al* 2009 Improved-confinement plasmas at high temperature and high beta in the MST RFP *Nucl. Fusion* **49** 104020